Layer Structures 8. Poly(benzoxazole-ester)s with a Four-Layer or a Six-Layer Repeat Unit

Christoph Wutz, Sven Thomsen, Gert Schwarz, and Hans R. Kricheldorf*

Institut für Technische und Makromolekulare Chemie der Universität, Bundesstrasse 45, D-20146 Hamburg, Germany

Received April 15, 1997; Revised Manuscript Received July 9, 1997[⊗]

ABSTRACT: Two isomeric polyesters (**3a** and **3b**) were synthesized from 2-(4-hydroxyphenyl)benzoxazolecarboxylic acid, 1,12-dodecanediol, and tetraethylene glycol, so that an alternating sequence of four subunits was obtained. Both polyesters differ in their internal orientation of the benzoxazole units with the consequence that only one of them (**3a**) is liquid-crystalline forming an enantiotropic smectic-C phase. Furthermore, a third polyester (**4**) was prepared with an alternating sequence of six subunits using 4,4′-dimercaptobiphenyl as a third stiff building block. Both DSC and X-ray measurements confirm that all three polyesters form a crystalline solid state with a smectic type layer structure. Fiber pattern indicate that in the case of **3a** and **3b** the chains are tilted with an angle of about 45° relative to the layer planes, and the solid state corresponds to a smectic-H structure. In the case of **4** the chains are in upright position, although four subunits are identical with the repeat unit of **3b**. Therefore, the solidification of **4** may be understood as a self-assembling process. The thermal phase transitions were also characterized by synchrotron radiation measurements up to the isotropization temperature.

Introduction

The present work is a contribution to a broader study of polymers forming layer structures in the solid state. The layer may parallel the main chains (the so-called sanidic layer structures[1−5]) or form a more or less perpendicular array relative to the polymer chains. The latter kind of layer structures may be labeled smectic layer structures.[6] In this connection it should be emphasized that—in contrast to low molar mass LC-materials—only two smectic phases of the LC-main-chain polymers are liquid crystalline, namely smectic-A and smectic-C. All other types of smectic layer structures are either solid mesophases or crystalline phases. The question if a solid smectic layer structure should be called the mesophase or the crystalline phase depends on the degree of its three-dimensional order. A sharp borderline between both types of supramolecular order does not exist, and a clearcut experimental differentiation is frequently difficult.

The standard smectic layer structure consists of two different layers; the layer of the rigid mesogen and that of the flexible spacers. However, a layer structure is only formed, if one of the components is polar and the second one nonpolar.[7,8] The present work and the succeeding part of this series—dealing with polyimides of the structures **1a**, **1b**, **2**—were aimed at synthesis and characterization of more complex layer structures. In the present work dealing with the poly(benzoxazole ester)s, PBOEs **3a**,**b**, and **4**, the following questions should be studied. First, how does the subtle change of the internal dipole moments influence the properties in the case of **3a** versus **3b**? Second, does the copolyester **4** crystallize and is the rate of crystallization comparable with that of **3a** and **3b**? Third, is the layer structure of **4** similar to that of **3b**? Fourth, does the X-ray beam detect the long periodicity of **4**, including the six sublayers? Fifth, how similiar or different are the properties of **3a**, **3b** and **4** when compared to **1a**, **1b**, and **2**?

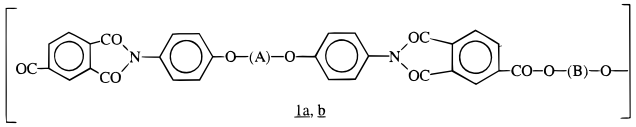

1a, b

a: (A) = $-(CH_2)_{12}-$, (B) = $(OCH_2CH_2)_4$

b: (A) = $(OCH_2CH_2)_4$, (B) = $-(CH_2)_{12}-$

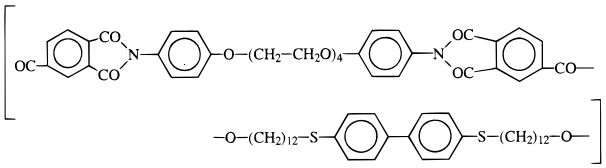

2

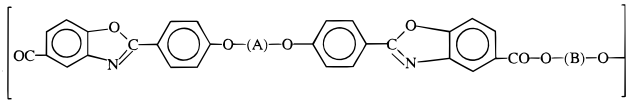

3a, b

a: (A) = $-(CH_2)_{12}-$, (B) = $-(CH_2CH_2O-)_4-$

b: (A) = $-(CH_2CH_2O-)_4-$, (B) = $-(CH_2)_{12}-$

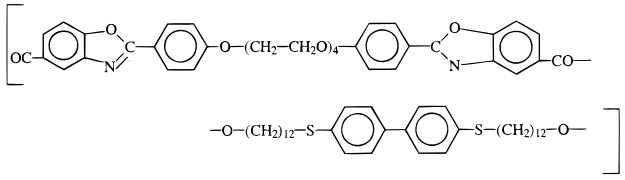

4

Experimental Section

Materials. 3-Amino-4-hydroxybenzoic acid, 4-hydroxybenzoic acid, thionyl chloride, and chlorotrimethylsilane were gifts of Bayer AG (Leverkusen, FRG) and were used as received. 1,12-Dibromododecane, tetraethylene glycol, 1-bromo-12-hydroxydodecane, biphenyl-4,4′-disulfonyl chloride and dimethyl sulfoxide (DMSO) were purchased from Aldrich Co. (Milwaukee, WI). Hexamethyldisilazane (HMDS) was purchased from Dynamite Nobel AG (Troisdorf, FRG).

[⊗] Abstract published in *Advance ACS Abstracts,* September 1, 1997.

S0024-9297(97)00511-1 CCC: $14.00

Table 1. Yields and Properties of Polyesters 3 and 4

polym no.	treatment	yield (%)	η_{inh}[a] (dl/g)	elem formula (fw)	elem anal.	% C	% H	% N	$CHCl_3$	DMF[c]	CH_2Cl_2 + TFA[d]	MSA[c]
3a	crude		0.75	$C_{48}H_{54}N_2O_{11}$	calcd	69.05	6.52	3.35				
	reprecip	91	0.83	(835.0)	found	68.88	6.63	3.49	++	+	++	++
					found	69.04	6.64	3.48	++	+	++	++
3b	crude		0.40	$C_{48}H_{54}N_2O_{11}$	calcd	69.05	6.52	3.35				
	reprecip	88	0.45	(835.0)	found	67.80	6.26	3.72	++	+	++	++
					found	68.67	6.52	3.61	++	+	++	++
4	crude		1.56	$C_{72}H_{86}N_2O_{13}S_2$	calcd	70.91	7.11	2.30				
	reprecip	94	1.68	(1219.6)	found	70.12	6.98	2.35	+	−	++	++
					found	70.48	7.08	2.27	+	−	++	++

[a] Measured at 20 °C with c = 2 g/L in CH_2Cl_2/TFA (volume ratio 4:1). [b] Determined for a potential concentration of 6 g/L at 25 °C. [c] DMF = dimethylformamide; MSA = methanesulfonic acid. [d] Volume ratio 4:1.

2-(4-Hydroxyphenyl)benzoxazole-5-carboxylic acid (5). This monomer (no mp, dec >300 °C) was prepared from 4-acetoxybenzoyl chloride and trisilylated 3-amino-4-hydroxybenzoic acid as described previously.[9,10]

1,12-Bis((5-carboxybenzoxazolo)phenoxy)dodecane (6a). 2-(4-Hydroxyphenyl)benzoxazole-5-carboxylic acid (**5**, 0.1 mol) was dissolved in a mixture of NaOH (0.25 mol), water (200 mL), and DMSO (200 mL). At 80 °C a solution of 1,12-dibromododecane (50 mmol) in DMSO (50 mL) was added dropwise with stirring. The reaction was stirred at 80 °C for 10 h and after addition of 50 mmol NaOH for another 10 h at 120 °C. The cold reaction mixture was poured into water and acidified with concentrated HCl to a pH of 1. The precipitated product was filtered off, washed with water, and dried in vacuo. Finally, it was recrystallized from dimethylformamide/water and dried over P_4O_{10} in vacuo: yield 43%; mp 300 °C (DSC). Anal. Calcd for $C_{40}H_{40}N_2O_6$ (676.8): C, 70.99; H, 5.96; N, 4.14. Found: C, 69.93; H, 6.06; N, 4.01.

^{1}H NMR (DMSO-d_6/TMS): δ = 1.28 (bs, 12 H), 1.74 (t, 4H), 4.78 (t, 4H), 7.12 (d, 4H), 7.92 (dd, 4H), 8.12 (d, 4H), 8.24 (s, 2H), 13.5 (bs, 2H) ppm.

1,12-Bis((5-(chlorocarbonyl)benzoxazolo)phenoxy)-dodecane (6c). The finely ground dicarboxylic acid **6a** (40 mmol) was refluxed for 3 h in a mixture of HMDS (150 mL) and xylene (250 mL). The volative reactants were then evaporated in vacuo and the residue (**6b**) was dried in a vacuum of 10^{-1} m bar. The dry residue was refluxed in a mixture of toluene (350 mL) and thionyl chloride (200 mL) for 3 h. The solvent and excess $SOCl_2$ were then evaporated in vacuo, and the residue was dissolved in dry toluene (200 mL) and dried again. This procedure was repeated to remove all thionyl chloride. The remaining crude product (yield 94%, mp 152−154 °C) was used for the sythesis of **6d** without further purification.

^{1}H NMR ($CDCl_3$/TMS): δ = 1.32 (bs, 12 H), 1.83 (t, 4H), 4.05 (t, 4H), 7.02 (d, 4H), 7.61 (d, 2H), 8.07-8.23 (m, 6H), 8.53 (d, 2H) ppm.

1,12-Bis((5-(methoxycarbonyl)benzoxazolo)phenoxy)-dodecane (6d). The dicarboxylic acid dichloride **6c** (40 mmol) was dissolved in a mixture of dry methanol (250 mL) and pyridine (80 mmol) and refluxed for 3 h. After being cooled with ice, the precipitated product was filtered off, washed with cold methanol, recrystallized from chloroform/ligroin, and dried at 80 °C in vacuo: yield 83%; mp 172−174 °C. Anal. Calcd for $C_{42}H_{44}N_2O_8$ (704.82): C, 71.57; H, 6.29; N, 3.97. Found: C, 70.98; H, 6.43; N, 4.06.

^{1}H NMR ($CDCl_3$/TMS): δ = 1.32 (bs, 12 H), 1.67 (t, 4H), 3.96 (s, 6H), 4.04 (t, 4H), 7.03 (d, 4H), 7.57 (d, 2H), 8.07 (dd, 2H), 8.18 (d, 4H) ppm.

Tetraethylene Glycol Bis((5-carboxybenzoxazolo)phenyl) Ether (7a). 2-(4-Hydroxyphenyl)benzoxazole-5-carboxylic acid (0.1 mol) was alkylated with the ditosylate of tetraethylene glycol (50 mmol) as described above for **6a**: yield 42%; no mp because of decomposition.

Anal. Calcd for $C_{36}H_{32}N_2O_{11}$ (668.6): C, 64.66; H, 4.86; N, 4.19. Found: C, 64.27; H, 4.81; N, 4.22.

^{1}H NMR (DMSO-d_6/TMS): δ = 3.57 (s, 8H), 3.75 (bs, 4H), 4.16 (bs, 4H), 7.09 (d, 4H), 7.80 (dd, 4H), 8.05 (d, 4H), 8.20 (d, 2H), 13.00 (bs, 2DH) ppm.

Tetraethylene Glycol Bis((5-(chlorocarbonyl)benzoxazolo)phenyl) Ether (7c). The dicarboxylic acid **7a** (40 mmol) was successively treated with HMDS and thionylchloride as described above for **6c**. The crude product (yield 74%, mp 73−75 °C) was used for the synthesis of **7d** without additional purification.

^{1}H NMR ($CDCl_3$/TMS): δ = 3.75 (s, 8H), 3.94 (t, 4H), 7.02 (d, 4H), 7.56 (d, 2H), 8.07 (dd, 6H), 8.45 (d, 2H) ppm.

Tetraethylene Glycol Bis((5-(methoxycarbonyl)benzoxazolo)phenyl) Ether (7d). The dicarboxylic acid chloride **7c** (20 mmol) was reacted with dry methanol and pyridine as described for **6d**: yield 72%; mp 123−125 °C. Anal. Calcd for $C_{38}H_{36}N_2O_{11}$ (696.7): C, 65.51; H, 5.21; N, 4.02. Found: C, 64.99; H, 4.96; N, 4.36.

^{1}H NMR ($CDCl_3$/TMS): δ = 3.74 (s, 8 H), 3.95 (m, 10H), 4.20 (t, 4H), 7.03 (d, 4H), 7.53 (d, 2H), 8.10 (m, 6H), 8.38 (d, 2H) ppm.

4,4′-Bis((12-hydroxydodecyl)thio)biphenyl (8). At first 4,4′-dimercaptobiphenyl[12] (mp 179−181 °C) was prepared from commercial 4,4′-bis(dichlorosulfonyl)biphenyl with $LiAlH_4$ in tetrahydrofuran. 4,4′-Dimercaptobiphenyl (10 mmol) was then dissolved in a deoxygenated solution of sodium (20 mmol) in dry ethanol (160 mL). A solution of 12-bromododecanol (20 mmol) in dry ethanol (60 mL) was added dropwise with stirring. The reaction mixture was refluxed for 3 h under a slow stream of nitrogen. After the reaction mixture was cooled, it was poured into cold water, and the precipitated product was isolated by filtration, washed with water, and dried at 80 °C in vacuo: yield 94%, mp 157−159 °C.

Anal. Calcd for $C_{36}H_{58}O_2S_2$ (587.0): C, 73.66; H, 9.96. Found: C, 73.97; H, 9.88.

^{1}H NMR ($CDCl_3$/TMS + 5 vol % trifluoroacetic acid): δ = 1.29 (bs, 32H), 1.69 (t, 4H), 2.98 (t, 4H), 4.37 (t, 4H), 7.45 (dd, 8H) ppm.

Polycondensations. The dimethyl ester (**6d** or **7d**, 5 mmol), a diol (5 mmol) and dibutyltin oxide (10 mg) were weighed into a cyclindrical glass reactor equipped with a mechanical stirrer and gas-inlet and gas-outlet tubes. The reactor was placed into a metal bath preheated to 150 °C. The temperature was rapidly raised to 200 °C. Afterward, the temperature was raised in steps of 10 °C over a period of 6 h up to final reaction temperature of 260 °C. Vacuum was applied for additional 0.5 h. The cold polyester was then dissolved in a mixture of CH_2Cl_2 and trifluoroacetic acid (volume ratio 4:1), precipitated into cold methanol, and dried at 80 °C in vacuo. The yields and some properties are listed in Table 1.

Measurements. The inherent viscosities were measured with an automated Ubbelohde viscometer thermostated at 20 °C.

The DSC measurements were conducted with a Perkin Elmer DSC-7 in aluminum pans under nitrogen.

The 100 MHz ^{1}H NMR spectra were recorded with a Bruker AC-100 FT NMR spectrometer in 5 mm o.d. sample tubes.

The WAXS powder patterns were recorded with a Siemens D-500 diffractometer using Ni-filtered Cu Kα radiation. The synchrotron radiation measurements were conducted with a wavelength of 1.50 Å at HASYLAB, (DESY, Hamburg, FRG) using an one-dimensional detector and a heating rate of 10 °C/min and 30 s acquisition time. The temperature specified for each frame is averaged over 30 s (5 °C).

Results and Discussion

Syntheses. The poly(benzoxazole-ester)s, PBOE's, **3a** and **3b** were prepared by polycondensation of the

dimethyl esters **6b** with tetraethylene glycol and **7d** with 1,12-dodecandediol. The dimethyl ester **6d** was synthesized by the reaction sequence shown in eqs 1−4.

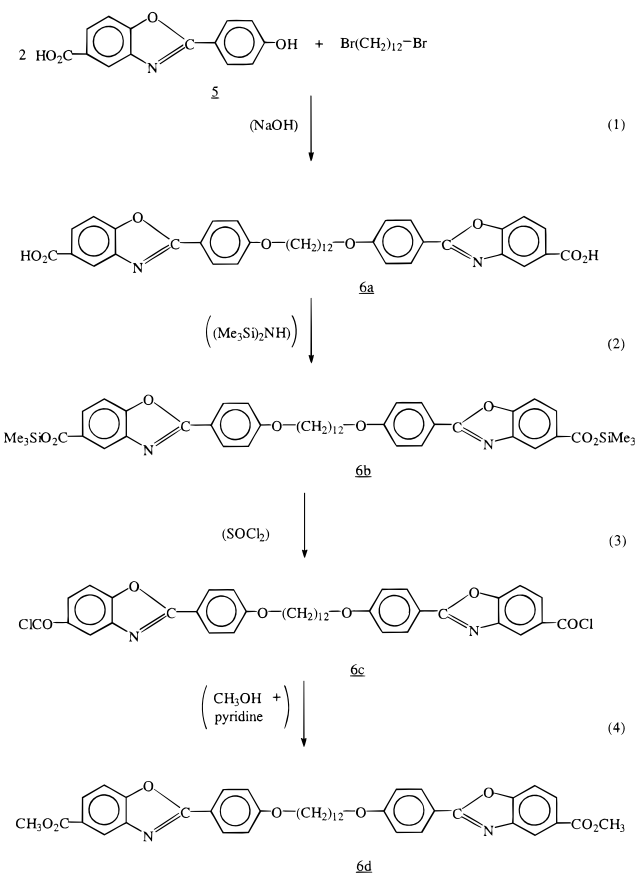

2-(4-Hydroxyphenyl)benzoxazole-5-carboxylic acid (**5**), which served as starting material for all three PBOE's, was obtained from silylated 3-amino-4-hydroxybenzoic acid and 4-acetoxybenzoyl chlorides as described previously.[9,10] Since benzoxazoles are stable under alkaline conditions the hydroxy acid **5** was directly alkylated with 1,12-dibromododecane in the presence of aqueous sodium hydroxide. The esterification of the dicarboxylic acid **6a** was conducted in a manner to avoid acidic reaction conditions, because the benzoxazole ring is sensitive to acidic cleavage. The silylation of carboxylic acid is an almost quantitative reaction, and the chlorination of trimethylsilyl esters avoids the formation of free HCl and proceeds under milder conditions than the chlorination of the free carboxylic acids.

The synthesis of the dimethyl ester **7d** was conducted analogously. The 2-(4-hydroxyphenyl)benzoxazole-5-carboxylic acid **5** was alkylated with the ditosylate of tetraethylene glycol, which is a commercial product. The resulting dicarboxylic acid **7a** was then transformed into its dimethyl-ester **7d** via **7b** and **7c**. The diol **8** was

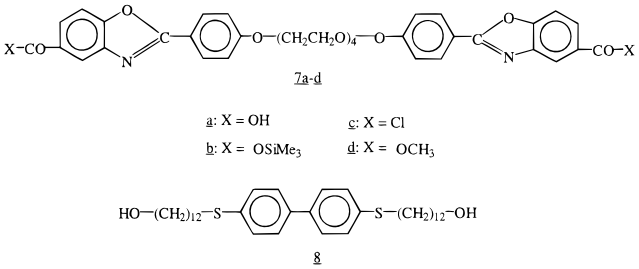

prepared by the reaction of 12-bromododecanol with 4,4′-dimercaptobiphenyl which was synthesized by the reaction of commercial 4,4′-bis(dichlorosulfonyl)biphenyl with lithium aluminium hydride alkylation of 4,4′-dimercaptobiphenyl with 12-bromo-1-dodecanol as described previously.[2] The PBOE **4** was then prepared from the dimethyl ester **7d** and diol **8**. All polycondensations were conducted in bulk at temperatures up to 260 °C using dibutyltin oxide as transesterification catalyst. The yields and several properties of the PBOE's **3a**, **3b**, and **4** are summarized in Table 1 whereas the phase transitions and x-ray data are compiled in Table 2.

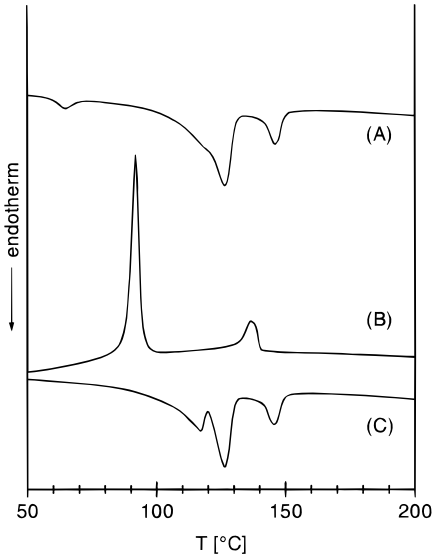

Figure 1. DSC measurements (heating and cooling rate 10 °C/min) of PBOE **3a** (dried at 80 °C): (A) first heating; (B) first cooling; (C) second heating.

Properties of PBOE 3a. DSC measurements of PBOE **3a** (and **3b**) dried at 80 °C were conducted at a heating and cooling rate of 10 °C/min (Figure 1). The first heating curve exhibits the glass transition at 56 °C and two endotherms at 127, and 146 °C. Upon cooling, two exotherms appear at 137, and 92 °C, respectively. In the second heating trace a third endotherm appears at 117 °C. Optical microscopy with crossed polarizers reveal the formation of a smectic LC phase above the endotherm at 127 °C which vanishes above the third endotherm (finally at 150 °C) which represents the isotropization process. Upon cooling at −10 °C/min, the smectic phase is formed at about 140 °C and extends down to 90−100 °C. Regardless of the heating and cooling rate the LC melt displays a "sandy texture" which slowly developes into a kind of schlieren texture upon long annealing (Figure 2). The typical bâtonnets or fan-shaped textures of a smectic-A phase have never been observed, and the schlieren were highly viscous in contrast to those of a nematic phase. Therefore, the optical microscopy suggests the formation of a smectic-C phase.

Time-resolved X-ray measurements employing synchrotron radiation were performed detecting the wide angle scattering (WAXS) (Figure 3) and the middle angle scattering (MAXS) (Figure 4) simultaneously. The integral intensities of the reflections are depicted in Figure 5 as a function of the temperature. Upon heating, the WAXS reflections become weaker over a wide temperature range due to partial melting of the smaller crystals. Meanwhile, the MAXS reflection at $2\theta = 4.4°$ increases, indicating that the loss of lateral interactions allows the mesogens an improvement of the layered ordering.

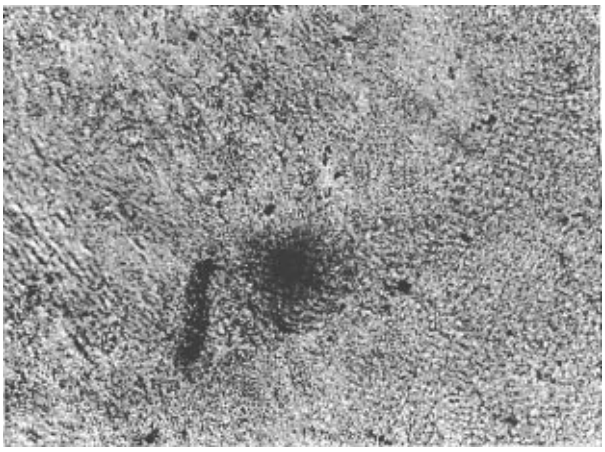

Figure 2. Texture of PBOE **3a** obtained upon slow cooling from the isotropic melt with 1 °C/min and subsequent holding at 140 °C for 4 h.

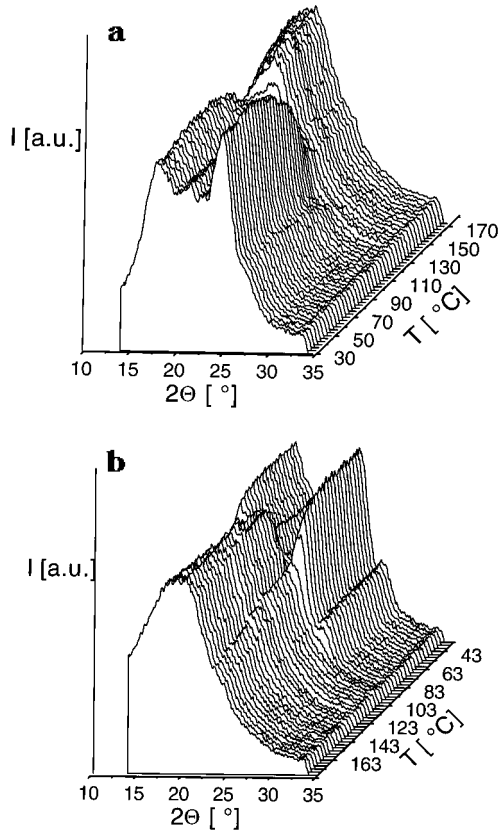

Figure 3. Change of WAXS of PBOE **3a** during the (A) first heating with 10 °C/min and (B) the first cooling at 10 °C/min.

Both the WAXS reflections and the MAXS reflections at $2\theta = 4.4$ and 2.3° vanish at 130 °C. However, a weak MAXS reflection at $2\theta = 4.0°$ persists up to a temperature of 150 °C at which isotropization is observed by optical microscopy. Upon cooling of this layer, the reflection at 4.0° reappears below 140 °C (Figure 4). Clearly, this MAXS reflection in absence of crystal reflections indicates the layer structure of an enatiotropic smectic LC phase.

The scattering angle of $2\theta = 4.0°$ corresponding to a d-spacing of 22 Å cannot be correlated to the full length of the repeating unit, which has been calculated to be on the order of 54 ± 1 Å. This calculation was carried out by computer modeling with a force field program assuming a 1:1 ratio of gauche and trans conformations in both spacers. The X-ray scattering detects the fluctuations of the electron density which are large between mesogen and spacer layer irrespective of the

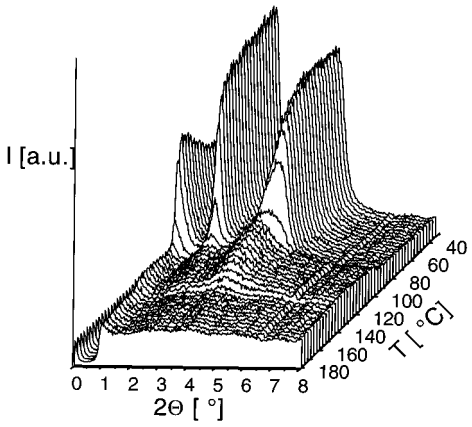

Figure 4. Change of MAXS of PBOE **3a** during the first cooling at 10 °C/min.

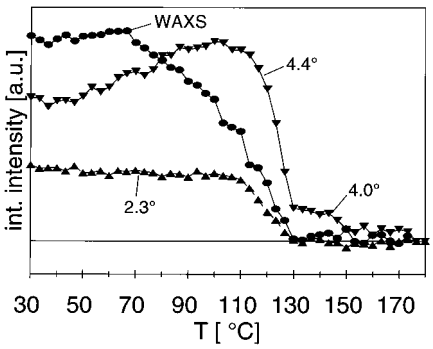

Figure 5. Integral intensities of all the WAXS reflections and the MAXS reflections of PBOE **3a** as a function of temperature during heating at 10 °C/min.

type of spacer. Thus, the MAXS reflection can be caused by the layer periodicity of only one mesogen and one spacer. Furthermore, a tilting of the chains with respect to the layer plane by an angle on the order of 40° have to be assumed, in agreement with the definition of a smectic-C phase.

This interpretation is supported by the X-ray data of the solid state. The MAXS reflections of **3a** at $2\theta = 4.4°$ and 2.3° (Figure 4) correspond to *d*-spacings of 20 and 38 Å, respectively. It is unlikely that the reflections represent the first- and second-order reflections of the same layer, because the 4.4° reflection has a higher intensity than the 2.3° reflection and its intensity increases upon annealing up to 100 °C while the other remains constant. Obviously, the 20 Å reflection is the analog of the 22 Å reflection observed for the melt and represents a layer consisting of one mesogen and one spacer in a slightly less tilted array. It may be assumed that the reflection is dominated by the layers containing alkane spacers (d_1) (Figure 6) because their electron density is lower compared to the oligo(ethylene oxide) spacer, and thus, the contrast to the mesogen is greater.

On the basis of these assumptions it is reasonable to attribute the 38 Å reflection to a super lattice corresponding to the periodicity of the full repeat unit (d_3). This *d*-spacing is not necessarily twice as high as the 20 Å of the sub layer d_1, because it is well known that oligo- and poly(ethylene oxide) prefer more gauche conformations than alkane chains at identical temperature, so that the sublayer d_2 may be slightly shorter than d_1 (see Figure 6).

This interpretation is confirmed by the X-ray fiber pattern of **3a** in Figure 7 which displays an eight-point pattern for the MAXS reflections. Assuming the chains to be oriented preferably parallel to the fiber direction, the azimuthal splitting of the reflections indicates a

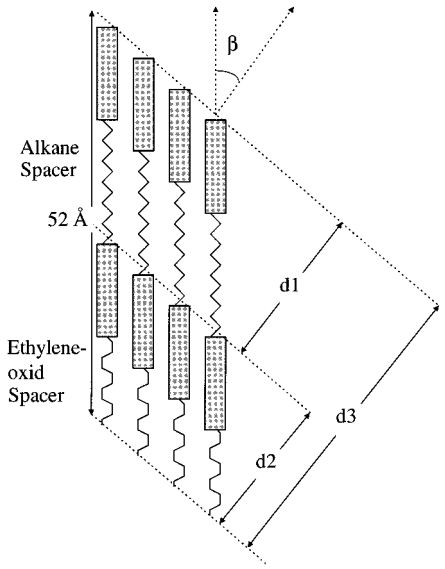

Figure 6. Scheme of the tilted layer structure of the PBOEs **3a** and **3b**.

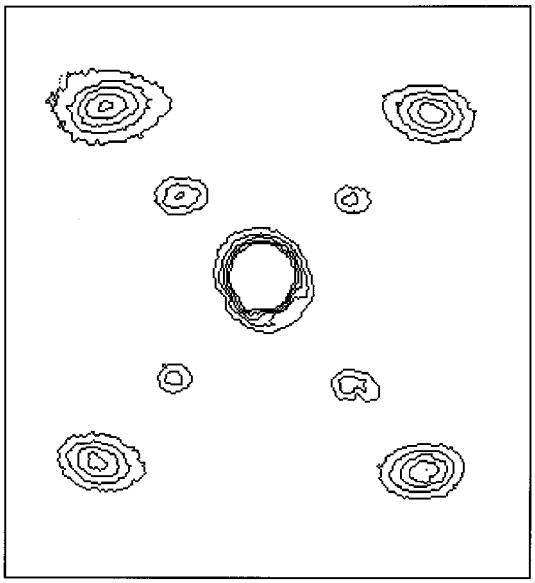

Figure 7. X-ray fiber pattern of PBOE **3a**.

tilting of the chains of $\beta = 43°$ with respect to the normal smectic layer plane within both layer structures.

From the meridional scattering angle of the MAXS reflections, the *d*-spacings in fiber direction, which are identical with the lengths of the repeat units, are calculated to be 52 and 27 Å, respectively. This result is in good agreement with the computer modeling, proving the assumption of 1:1 ratio of gauche and trans conformations to be valid for the alkane spacer, whereas for the oligo(ethylene oxide) spacer a higher fraction of gauche conformations should be accounted for.

Taken together, optical microscopy and DSC and X-ray measurements allow a consistent interpretation of the phase behavior of PBOE **3a**. The solid state may be described as a crystalline solid with a smectic-type layer structure (smectic-H) with a tilt angle of $\beta = 43°$. Upon heating, an enantiotropic smectic-C phase is formed. The loss of lateral interactions allows the mesogens to change their orientation with respect to the layer plane. The layer thickness of 22 Å corresponds to a tilt angle of $\beta = 35°$. Although the mesogens take the thermodynamically most favorable orientation in this way, the layer structure is disturbed severely and the correlation of the super lattice is almost lost.

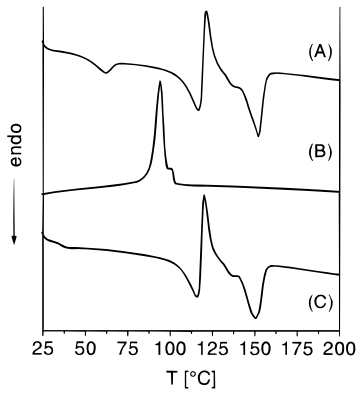

Figure 8. DSC measurements (heating and cooling rate 10 °C/min) of PBOE **3b**: (A) first heating; (B) first cooling; (C) second heating.

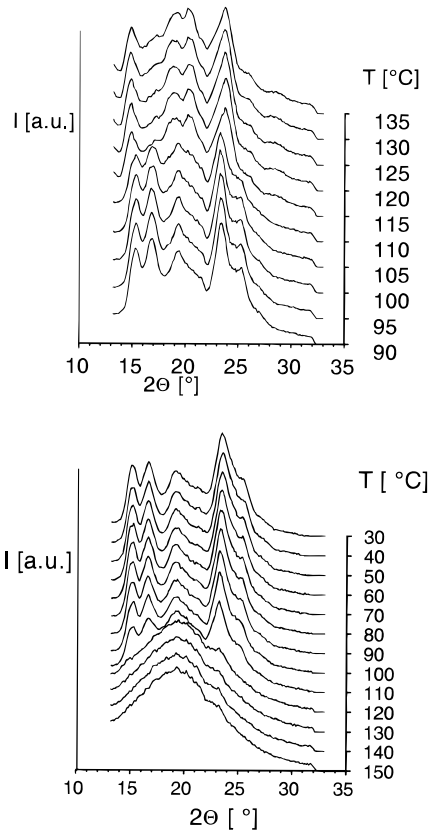

Figure 9. Change of WAXS of PBOE **3b** during the first heating (A) and cooling (B) at 10 °C/min.

Properties of PBOE 3b. The DSC measurements of **3b** again display in the first heating curve the glass transition at 52 °C and two endotherms at 115 and 151 °C (Figure 8). However, the first endotherm is followed by an exotherm indicating a recrystallization process. The endotherm at 151 °C was proved by optical microscopy to be the melting endotherm, and no liquid crystalline phase was found. The synchrotron radiation measurements of the WAXS (Figure 9) and MAXS (Figure 10) clearly indicate a change of the crystal structure at 115 °C. The low temperature modification (I) is characterized by WAXS reflections at $2\theta = 15.4$, 16.8, 19.7, and 26° in combination with two MAXS reflections at $2\theta = 2.0$ and 4.1° which can be attributed to a layer structure with d-spacings of 45 and 22 Å, respectively. The higher temperature modification (II) exhibits WAXS reflections at $2\theta = 15.2$, 19.0, 20.8, and 24.5° and a MAXS reflection at $2\theta = 5.85°$ corresponding to a layer spacing of 15 Å. All these reflections disappear above the T_m of 150 °C. The transition from modification I to

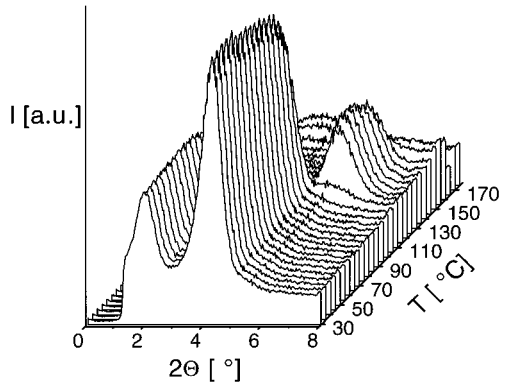

Figure 10. Change of MAXS of PBOE **3b** during the first heating at 10 °C/min.

Figure 11. X-ray fiber pattern of PBOE **3b**.

modification II is irreversible. Thus, modification II is thermodynamically stable while modification I is metastable. Upon cooling at 10 °C/min, modification I is formed predominantly due to its faster kinetics of formation. The ratio of modifications I and II formed upon cooling depends on the cooling rate, but the reheating produces again exclusively the thermodynamically stable modification II. Short annealing at temperatures between 125 and 135 °C has the same effect. Modification I disappears, and modification II is exclusively formed. A DSC heating curve of such an annealed sample displays only one endotherm at 150 °C.

These observations demonstate that the thermal properties and phase behavior of **3b** differ largely from those of **3a** despite a nearly identical chemical structure.

The dimensions of the layer structure of modification I of **3b** resemble closely those of the solid state of **3a**. Accordingly, **3b** also forms a smectic-H phase with strongly tilted repeat units. This interpretation is confirmed by the X-ray fiber pattern displayed in Figure 11. The MAXS exhibits a four-point pattern at $2\theta = 4.1°$ while the main WAXS reflections occur at the equator, indicating a tilt angle of $\beta = 40°$ of the mesogens with respect to the normal of the smectic layer plane in modification I. The second MAXS reflection at $2\theta = 2.0°$ is faded out by the beamstop in the fiber patter. A layer distance in fiber direction corresponding to the length of the repeat unit can be calculated from the meridional scattering angle and amounts to 28 Å, which is in good agreement with the d_1-spacing of **3a**.

However, a straightforward interpretation of the X-ray reflections of modfication II cannot be offered at this time.

Properties of PBOE 4. The DSC traces (Figure 12) of PBOE **4** and the optical microscopy observations indicate that the thermal properties of **4** are somewhat simpler than those of **3a** and **3b**. A LC-phase was not detected, nor was any change of the crystal modification observed. The endotherm upon heating at 127 °C and the corresponding exotherm upon cooling at 100 °C represent the melting/crystallization process. The synchrotron radiation measurements (Figure 13) support the above interpretation. All reflections disappear at the melting temperature of 130 ± 1 °C and neither a shift of their positions nor a significant change of their intensities can be observed.

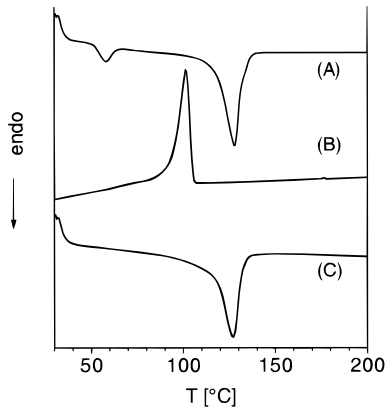

Figure 12. DSC measurements (heating and cooling rate 20 °C/min) of PBOE **4**: (A) first heating; (B) first cooling; (C) second heating.

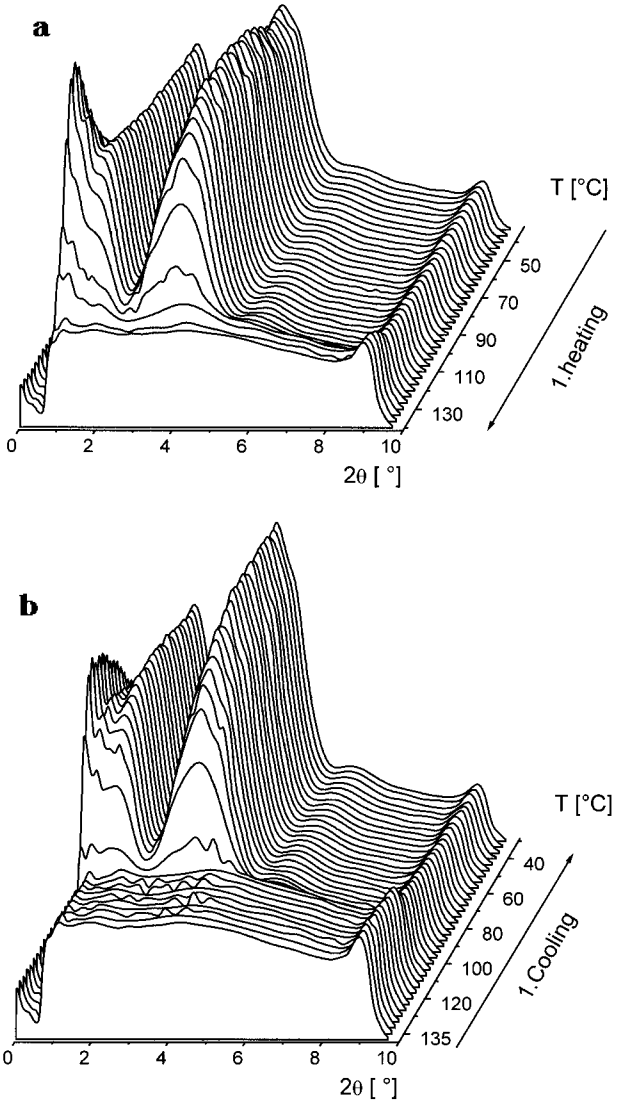

Figure 13. Change of MAXS of PBOE **4** during the first heating (A) and cooling (B) at 10 °C/min.

The X-ray fiber pattern of PBOE **4** in Figure 14 exhibits only meridional reflections, indicating that the mesogens are not tilted. The layer reflection at $2\theta = 1.6°$ corresponds to a d-spacing of 55 Å. The second-order reflection is detectable at $2\theta = 3.2°$. The third reflection at $2\theta = 4.4°$ indicates another layer structure with a spacing of $d = 20$ Å which cannot be attributed to a molecular repeat unit satisfactorally. A fourth weak reflection at $2\theta =$

Table 2. Phase Transitions and X-ray Reflections of the PBOEs 3a, 3b, and 4

		transtn temp[a] (°C)					MAR		
polym no.	T_g[a] (°C)	heating		cooling		form	2θ (deg)	d (Å)	WAXS 2θ (deg)
3a	56	$T_{C\rightarrow LC}$	$T_{LC\rightarrow i}$	$T_{i\rightarrow LC}$	$T_{LC\rightarrow C}$	C	4.4/2.3	20/38	17.7, 21.2, 24.5, 27.4
		127 (117)	146	137	92	LC	4.0	22	
3b	52	$T_{CI\rightarrow CII}$	$T_{CII\rightarrow i}$		$T_{i\rightarrow CI}$	(I)	4.1/2.0	22/45	15.4, 16.8, 19.7, 26.0
		115	151		94	(II)	5.85	15	15.2, 19.0, 20.8, 24.5
4	52		$T_{C\rightarrow i}$		$T_{i\rightarrow C}$		1.6/4.4	55/20	19.7, 23.0, 28.0
			127		101				

[a] From DSC measurements with a heating/cooling rate of 20 °C/min.

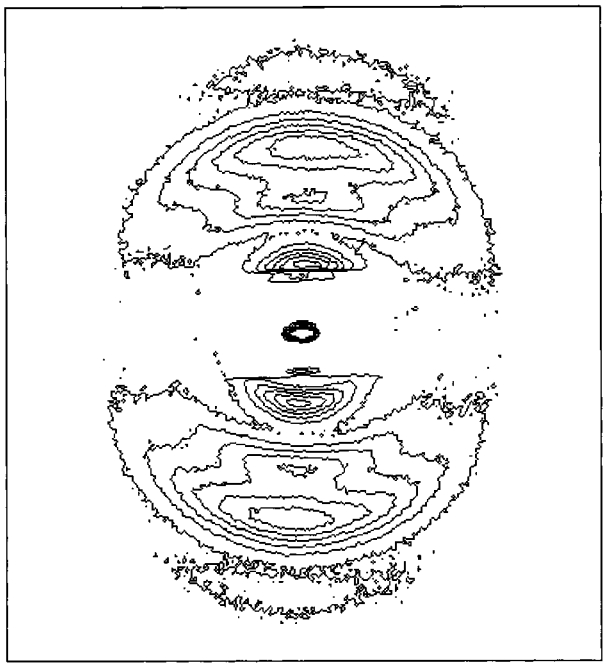

Figure 14. X-ray fiber pattern of PBOE **4**.

6.3° should be assigned as the fourth order of the 55 Å reflection.

It is difficult to attribute the layer spacings calculated from the MAXS to the complex molecular structure of PBOE **4**. Obviously, there is no correlation within the layer structure of the full repeat unit which has a length of 77−85 Å depending on the assumed spacer conformation. On the other hand, the two benzoxazole units together with two spacers seem to form a layer structure comparable to those of **3a** and **3b**, irrespective of the adjecent biphenyl moiety, and this four-layer structure corresponds to the measured *d*-spacing of 55 Å.

The PBOE **4** differs from the PBOEs **3a** and **3b** in thermal behavior and chain packing. The crystalline solid state has an orthogonal smectic layer structure (e.g. smectic-E) without a correlation of the layer structure extended over the full repeat unit.

Conclusion

The present study of three polyesters containing regular sequences of benzoxazole mesogens and flexible spacers allow the following conclusions. All three polyesters crystallize rapidly forming well ordered layer structures, despite the complexity of the chemical structure in the case of PBOE **4**. Obviously, the regular pattern of polar and nonpolar, aromatic and aliphatic building blocks allows a rapid "self-assembly" of neighboring chains. The sensitivity of the resulting layer structure to slight changes in the chemical structure is documented by the finding that **3a** and **3b** show quite different phase behaviors, despite their isomeric repeat units. A liquid-crystalline phase (smectic-C) was found only in the case of **3a**, whereas **3b** undergoes a solid−solid transition between two higher ordered smectic-H phases. Surprisingly, the polyester with the most complex chemical structure (PBOE **4**) shows the simplest phase behavior, namely one melting/crystallization transition. Furthermore, PBOE **4** also differs from **3a** and **3b** by adopting an upright orientation of the repeat units relative to the layer planes corresponding to a smectic-E phase. This difference is interesting and unexpected because four subunits of **4** are identical with the repeat unit of **3b**. Therefore, the different chain packing reflects a strong influence of the two additional subunits (biphenyl and one more dodecamethylene spacer). Obviously, both the nucleation and the crystallization do not proceed in steps involving sublayers but a coordination of longer sequences (at least one full repeat unit) of neighboring chains. Therefore, the solidification of **4** merits the label "self-assembly". The formation of a super layer consisting of six sublayers has the consequence that the correlation of the X-ray scattering is lost over the super lattice of the full repeat unit but reflects only sublayers.

When compared to the analogous poly(ester-imide)s **1a**, **1b**, and **2** the PBOEs have the formation of crystalline smectic layer structures in common. However, the poly(ester−imide) **1a**, the structural analog of PBOE **3a**, does not form a LC phase as demonstrated in the next part of this series.[12]

References and Notes

(1) Herrmann-Schönherr, D.; Wendorff, J. H.; Ringsdorf, H.; Tschirner, P, *Makromol. Chem. Rapid Commun.* **1987**, *7*, 761.
(2) Ballauff, M. *Angew. Chem.* **1989**, *101*, 761.
(3) Adam, A.; Spiess, H. W. *Makromol. Chem. Rapid Commun.* **1990**, *11*, 249.
(4) Stern, R.; Ballauff, M.; Lieser, G.; Wegner, G. *Polymer* **1996**, *32*, 2096.
(5) Kricheldorf, H. R.; Domschke, A. *Macromolecules* **1996**, *29*, 1327.
(6) Gray, J.; Goodby, W. G. *Smectic Liquid Crystals*; Leonard Hill: New York, 1984.
(7) Kricheldorf, H. R.; Schwarz, G.; de Abajo, J.; de la Campa, J. *Polymer* **1991**, *32*, 942.
(8) Kricheldorf, H. R.; Schwarz, G.; Berghahn, M.; de Abajo, J.; de la Campa, J. *Macromolecules* **1994**, *27*, 2540.
(9) Kricheldorf, H. R.; Thomsen, S. A. *J. Polym. Sci., Part A: Polym. Chem.* **1991**, *29*, 1751.
(10) Kricheldorf, H. R.; Thomsen, S. A. *Makromol. Chem.* **1992**, *193*, 2467.
(11) Gabriel, S.; Deutsch, A. *Ber. Dtsch. Chem Ges.* **1880**, *13*, 390.
(12) Schwarz, G.; Thomsen, S. A.; Wutz, C.; Kricheldorf, H. R. *Acta Polym.*, submitted for publication.

MA970511E